Infrared signature of the superconducting state in $Pr_{2-x}Ce_xCuO_4$

A. Zimmers, R. P. S. M. Lobo,* and N. Bontemps
Laboratoire de Physique du Solide (UPR 5 CNRS) ESPCI, 10 Rue Vauquelin 75231 Paris, France

C. C. Homes
Department of Physics, Brookhaven National Laboratory, Upton, New York 11973, USA

M. C. Barr, Y. Dagan, and R. L. Greene
Center for Superconductivity Research, Department of Physics, University of Maryland, College Park, Maryland 20742, USA
(Received 14 May 2004; revised manuscript received 9 July 2004; published 26 October 2004)

We measured the far infrared reflectivity of two superconducting $Pr_{2-x}Ce_xCuO_4$ films above and below T_c. The reflectivity in the superconducting state increases and the optical conductivity drops at low energies, in agreement with the opening of a (possibly) anisotropic superconducting gap. The maximum energy of the gap scales roughly with T_c as $2\Delta_{max}/k_BT_c \approx 4.7$. We determined absolute values of the penetration depth at 5 K as $\lambda_{ab}=(3300\pm700)$ Å for $x=0.15$ and $\lambda_{ab}=(2000\pm300)$ Å for $x=0.17$. A spectral weight analysis shows that the Ferrell-Glover-Tinkham sum rule is satisfied at conventional low energy scales $\sim 4\Delta_{max}$.

DOI: 10.1103/PhysRevB.70.132502 PACS number(s): 74.25.Gz, 74.72.Jt

Since the discovery of high-T_c superconductivity, considerable efforts have been made to describe and understand the response of the superconducting phase. Over the years, measurements have been carried out in larger temperature and doping ranges, hoping to gain new insight into the problem.

The discovery of electron-doped cuprates[1,2] gave access to the mirror image of the hole doped phase diagram with respect to the Mott insulator state. Since then, significant work has been made looking for the differences and similarities in systems with either type of carrier.[3] The general phase diagram presents global symmetry, yet the magnetic properties show clear differences, the most obvious being the much broader antiferromagnetic phase on the electron doped side.

On the hole-doped side the main results from infrared spectroscopy can be summarized as: (i) in the normal state, indirect evidence of the pseudogap phase has come from analysis of the inverse quasiparticle lifetime $1/\tau(\omega)$, which is depleted over a range $\approx$100 meV;[4] (ii) the system evolves smoothly from the normal state into the superconducting state with no typical energy scaling with T_c;[5] (iii) for most dopings these materials are in the clean limit;[6] and (iv) a nonconventional pairing mechanism is supported by some evidence that high energy states contribute to the formation of the condensate in the underdoped regime.[7–9]

Recent studies above T_c, in the electron-doped side, have concluded through direct spectral weight analysis that a high energy partial gap opened in the normal state.[10–12] However very little is known about the optical properties in the superconducting state, most likely due to the low energy associated with the superconducting gap.[13–15] Indeed, most studies rely on the Raman scattering of $Nd_{2-x}Ce_xCuO_4$ (NCCO) and $Pr_{2-x}Ce_xCuO_4$ (PCCO) at optimal doping (maximum T_c) $x=0.15$.[17–19]

In this paper, we take advantage of the large surface and good homogeneity of PCCO films to explore the changes induced by superconductivity in the far-infrared spectra. Our data show an enhanced reflectivity at low frequencies when going into the superconducting state, on an energy scale entirely different from that of the normal state gap.[10–12] This feature is translated as a spectral weight loss in the real part of the optical conductivity. Comparing one overdoped to one optimally doped sample we show that the energy scale associated with the superconducting gap roughly scales with T_c.

Two PCCO films were epitaxially grown by pulsed-laser deposition on $SrTiO_3$ and annealed in reducing atmosphere.[20] The optimally doped sample is obtained with $x=0.15$, has $T_c=21$ K and is 3780 Å thick. The sample with $x=0.17$ is in the overdoped regime, has $T_c=15$ K and a thickness of 3750 Å. The critical temperatures were obtained by electrical transport and are defined by the zero resistance. Thin films are extremely homogeneous in the Ce concentration and their large surface to volume ratio makes them easy to anneal.

Near normal incidence infrared and visible reflectivity spectra were taken between 60 and 21000 cm^{-1} in a Bruker IFS 66v interferometer at ESPCI. These data were extended to the very far-infrared (10–200 cm^{-1}) at Brookhaven National Laboratory utilizing a Bruker IFS 113v interferometer. The films had an exposed area to the infrared light of about 5 mm in diameter. At ESPCI, gold mirrors were used as a reference below 10000 cm^{-1} and silver mirrors above 8000 cm^{-1}. The data are corrected for the absolute reflectivity of Au and Ag. The reflectivity measured at BNL uses an *in situ* overcoating of the sample by gold as a reference.[16] Measurements taken at ESPCI and at BNL agree within 0.2%, giving a rough estimate of the error in the reflectivity. The relative accuracy of the measurement (between two consecutive temperatures, for instance) is estimated to be better than 0.1%.

Data were taken at several temperatures in the whole spectral range but in this paper we are only going to compare the far-infrared spectrum (below 500 cm^{-1}) just above T_c to the one at 5 K. The normal state properties and the full spectral range are discussed elsewhere.[10]

To account for the substrate contributions we measured the reflectivity of $SrTiO_3$ at the same temperatures as those

selected to measure our samples. We then searched for a dielectric function for the film that describes the reflectivity of the whole system using a standard thin film model. This procedure has been successfully used to account for the temperature dependence of the substrate phonons (in particular the $SrTiO_3$ soft mode) and far infrared properties.[21] We fitted both films normal state reflectivities in the whole spectral range (20–21000 cm^{-1}) within 0.2%. The dielectric function thus obtained was utilized to generate the bulk reflectivities of PCCO above T_c. In both samples, it turns out that below 200 cm^{-1} the normal state bulk response is the same as the experimentally determined film reflectivity (within 0.2%) meaning that the substrate contribution is negligible in this low frequency range. As we discuss further, the superconducting transition is characterized by an increase of the low frequency reflectivity. The shape of this extra reflectivity is not trivial to simulate. However, as the superconducting state is more reflective than the normal state, it is safe to assume that the low frequency bulk and measured reflectivity are also identical in the superconducting state. In each film, beyond 100 cm^{-1}, the reflectivities of the normal and the superconducting state are identical, within the accuracy of the measurement, from 25 K, just above T_c, down to the lowest temperature.

The overall bulk reflectivity of PCCO can then be obtained by combining the measured data below 200 cm^{-1} to the bulk simulation above 100 cm^{-1}. Finally, we applied standard Kramers-Kronig analysis to such reconstructed spectra in order to extract the optical conductivity of PCCO. Below 20 cm^{-1} we used a Hagen-Rubens $(1-a\sqrt{\omega})$ extrapolation for the normal state reflectivity and a superconductor extrapolation $(1-b\omega^4)$ below T_c. Above 21000 cm^{-1} we used a constant up to 10^6 cm^{-1} followed by a free electron $1/\omega^4$ termination.

Figure 1 shows the real part of the optical conductivity (σ_1) for $x=0.15$ (top panel) and 0.17 (bottom panel). The insets in this figure show the measured far-infrared reflectivity. In all panels the dashed line is taken just above T_c and the solid line at 5 K. In both compounds the far infrared reflectivity increases, corresponding to a depletion in the superconducting σ_1 at low frequencies.

In Fig. 2 we plot the ratio between superconducting and normal reflectivity (left panel) and conductivity (right panel) for the $x=0.15$ (dashed line) and $x=0.17$ (solid line) samples. We note that there is an increase in the low energy reflectivity at 70 cm^{-1} for $x=0.15$ and 50 cm^{-1} for $x=0.17$. The corresponding decreases in the optical conductivity occurs at 90 cm^{-1} and 60 cm^{-1}.

In a *s*-wave BCS superconductor a rise in the low frequency reflectivity is associated with an isotropic superconducting gap (2Δ). However the BCS reflectivity is much flatter and closer to unity than what is seen in our data. Nevertheless, the reflectivity rise is compatible with the onset of an anisotropic gap. Indeed, the two strongest arguments against the observation of the gap in cuprates are (i) the energy range where the reflectivity increases does not vary with doping and (ii) cuprates are thought to be in the clean limit making the observation of a gap difficult. The first argument is clearly not applicable to our data. To

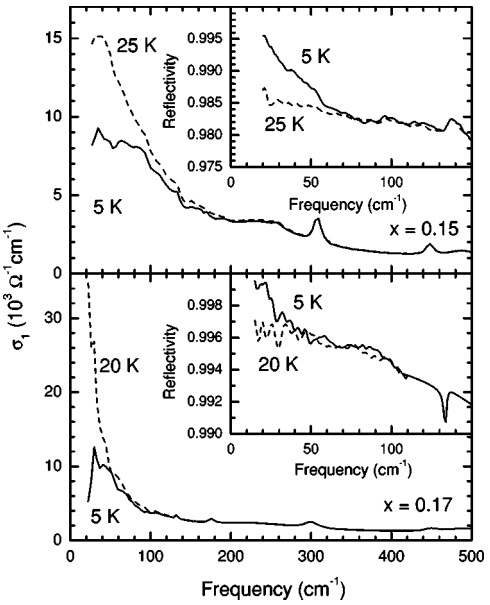

FIG. 1. Real part of the optical conductivity for the optimally (top panel) and overdoped (bottom panel) $Pr_{2-x}Ce_xCuO_4$. The insets show the far-infrared reflectivity for the respective samples. In all panels the dashed line corresponds to a temperature just above T_c and the solid line to 5 K.

counter the second point we can look at the low frequency scattering rate just above T_c. In the optimally doped sample we have $1/\tau(0)\approx 85$ cm^{-1} and in the overdoped material $1/\tau(0)\approx 30$ cm^{-1}. These values are of the same order of the frequency where the reflectivity increases. It is then reasonable to assign the reflectivity rise and the conductivity drop to the superconducting gap. In the absence of a specific model for such a gap, we can only estimate the maximum gap value from the frequencies where the low energy reflectivity or conductivity in the superconducting state differs from the ones above T_c. If we use the values obtained from σ_1 we have a $2\Delta_{max}/k_BT_c$ ratio of 6 for $x=0.15$ and 5.6 for $x=0.17$. This value is probably an overestimate of the gap energy. Considering the frequencies obtained from the reflectivity, the $2\Delta_{max}/k_BT_c$ ratio is 4.7 for both samples, in closer agreement to the values inferred from the Raman B_{2g} symmetry in NCCO samples.[17–19]

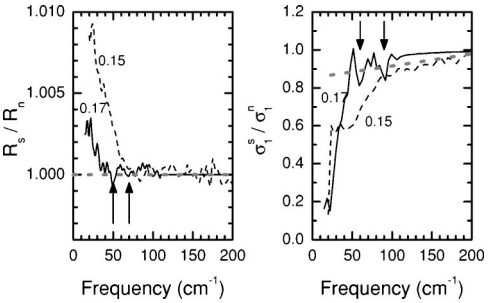

FIG. 2. Superconducting to normal state ratio of the reflectivity (left panel) and optical conductivity (right panel) in PCCO. The dashed line is for $x=0.15$ and the solid line for $x=0.17$. The dotted straight lines are guides for the eye representing the average high frequency behavior. The arrows indicate the frequency where this linear behavior breaks down.

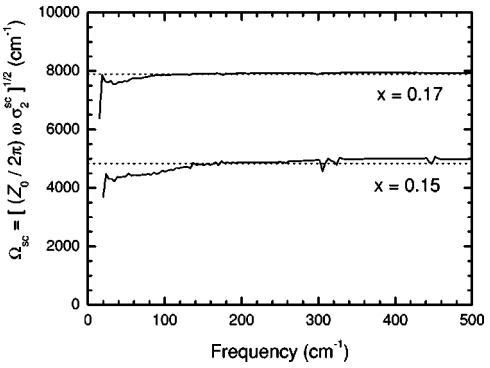

FIG. 3. Superconducting plasma frequency extracted from the $1/\omega$ component of σ_2 in the superconducting state. The dotted lines are the average values for Ω_{sc} between 20 and 500 cm^{-1}.

To further quantify the superconducting properties of PCCO, we looked at the *f*-sum rule. It follows from charge conservation and states that

$$\int_0^\infty \sigma_1(\omega')d\omega' = \frac{\pi^2}{Z_0}\frac{ne^2}{m}, \tag{1}$$

where $Z_0 \approx 377\ \Omega$ is the vacuum impedance, n the charge density, and e and m the electronic charge and mass, respectively.

Infinite conductivity in the superconducting state is represented by a $\delta(\omega)$ peak at the origin in σ_1. The *f*-sum rule then implies that the spectral weight of the $\delta(\omega)$ peak must come from finite frequencies, hence the decrease in σ_1. In fact, Ferrell, Glover, and Tinkham (FGT) (Refs. 22 and 23) have shown that the spectral weight lost at finites frequencies of σ_1 in the superconducting state is recovered in the superfluid weight.

To verify the FGT sum rule we need to determine the superfluid weight. One way to calculate it is to use the imaginary part σ_2 of the optical conductivity.[24] In the superconducting state one can write σ_1 as

$$\sigma_1(\omega) = \frac{\pi^2}{Z_0}\Omega_{sc}^2\delta(\omega) + \sigma_1'(\omega), \tag{2}$$

where Ω_{sc} is the superconducting plasma frequency. σ_2 then follows from Kramers-Kronig as

$$\sigma_2(\omega) = \frac{2\pi}{Z_0\omega}\Omega_{sc}^2 - \frac{2\omega}{\pi}\int_0^\infty \frac{\sigma_1'(\omega')}{\omega'^2 - \omega^2}d\omega' \tag{3}$$

and we define σ_2^{sc} as the first term on the right-hand side of Eq. (3).

Kramers-Kronig of the reflectivity data yield directly σ_1 and σ_2. Because σ_1 is obtained only for finite frequencies, it has no information on the $\delta(\omega)$ function and therefore equals σ_1'. We can thus apply Eq. (3) and calculate σ_2^{sc}.

Figure 3 shows that $\sqrt{\omega\sigma_2^{sc}}$ for both samples is indeed fairly constant below 500 cm^{-1} and corresponds to $\Omega_{sc} = (4800 \pm 1000)$ cm^{-1} for $x = 0.15$ and $\Omega_{sc} = (7900 \pm 750)$ cm^{-1} for $x = 0.17$. The contributions to errors in Ω_{sc} come from (i) the uncertainties in fitting the low frequency $\omega\sigma_2^{sc}$ to a constant value; and (ii) different extrapolations used in the Kramers-Kronig calculations. The absolute value of the superconducting penetration depth at 5K can be calculated using $\lambda_{ab} = (1/2\pi)\Omega_{sc}^{-1}$ and yield $\lambda_{ab} = (3300 \pm 700)$ Å for $x = 0.15$ and $\lambda_{ab} = (2000 \pm 300)$ Å for $x = 0.17$. These values are in good agreement with the ones obtained by microwave absorption.[25,26]

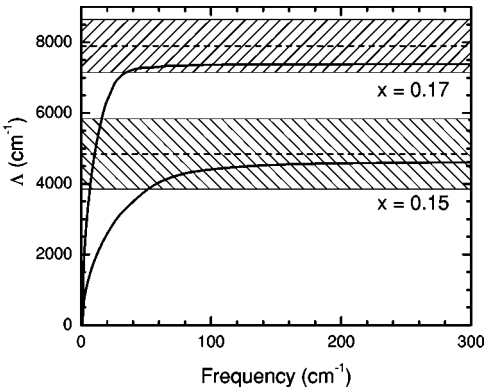

FIG. 4. Partial differential sum rule for optimally and overdoped PCCO calculated using Eq. (4). The dashed lines are the superconducting plasma frequencies calculated from Fig. 3. The shaded areas indicate the error in these values.

We can now verify the FGT sum rule by comparing the spectral weight lost in σ_1 to the superfluid weight calculated above. To do so, we define a partial differential sum rule

$$\Lambda^2(\omega) = \frac{Z_0}{\pi^2}\int_{0^+}^{\omega} [\sigma_1^N(\omega') - \sigma_1^S(\omega')]d\omega', \tag{4}$$

where the superscripts N and S refer to the normal and superconducting states, respectively. One should read $\Lambda(\omega)$ as the contribution from states up to ω to the superconducting plasma frequency, i.e., $\Omega_{sc} = \Lambda(\omega \to \infty)$.

Figure 4 shows $\Lambda(\omega)$ for both films. To correctly obtain $\Lambda(\omega)$, one must integrate from 0^+ but our data only go down to 20 cm^{-1}. To get the area between 0 and 20 cm^{-1}, we fitted the normal state σ_1 using a Drude peak. For lack of a good extrapolation, the superconducting σ_1 was set to 0 below 20 cm^{-1}. Inspection of Fig. 1 shows that this approximation is reasonable for the overdoped sample. However it will largely overestimate $\Lambda(\omega)$ in the optimally doped compound. In that case we used a constant extrapolation to zero frequency. The dashed lines in Fig. 4 are the superconducting plasma frequencies calculated from Fig. 3. The shaded areas indicate the error in these values.

Figure 4 is showing how far one must integrate the conductivity to obtain Ω_{sc} from $\Lambda(\omega)$. Within error bars the FGT sum rule is fulfilled in both samples below 200 cm^{-1} (25 meV). A similar analysis in underdoped $Bi_2Sr_2CaCu_2O_{8-\delta}$ shows that one must integrate Eq. (4) to very high energies (2 eV) in order to recover the spectral weight of the condensate.[7,8] A similar effect was also seen in

$YBa_2Cu_3O_{6.5}$ where the integration must be carried up to 0.5 eV to satisfy the FGT sum rule.[9] This energy range is characteristic of the boson spectrum responsible for the pairing mechanism, which led to the conclusion that the pairing mechanism was unconventional.[27–32] In our PCCO samples, Fig. 4 shows that the states contributing to the formation of the superfluid lie at energies comparable to the phonon spectrum.

The energy scale over which the condensate is recovered as well as the superconducting gap value are much smaller than the magnitude of the normal state (pseudo) gap observed around 100 meV.[10–12] This is in striking contrast with hole doped cuprates where the area loss in the real part of the conductivity, due to superconductivity, occurs over an energy scale which is similar to the one associated with the pseudogap state. This might imply that the normal state gap in electron doped cuprates has a different microscopic origin from the pseudogap in hole doped cuprates.

In conclusion, we have measured the optical conductivity of one optimally doped and one overdoped $Pr_{2-x}Ce_xCuO_4$ film. The reflectivity increase at low frequencies can be associated with the superconducting gap maximum and its value scales with T_c as $2\Delta_{\max} \approx 4.7 k_B T_c$. The superconducting penetration depth at 5 K was determined to be $\lambda_{ab} = (3300 \pm 700)$ Å for the optimally doped sample and $\lambda_{ab} = (2000 \pm 300)$ Å for the overdoped one. The partial differential sum rule shows that the superfluid condensate is built from states below 25 meV compatible with a more conventional low energy pairing mechanism.

The authors thank Dr. V.N. Kulkarni for RBS/Channeling measurements and C.P. Hill for help in the sample preparation. The work at University of Maryland was supported by NSF Grant No. DMR-0102350. The work at Brookhaven National Laboratory was supported by DOE under Contract No. DE-AC02-98CH10886.

*Electronic address: lobo@espci.fr

[1] Y. Tokura, H. Takagi, and S. Uchida, Nature (London) **337**, 345 (1989).
[2] H. Takagi, S. Uchida, and Y. Tokura, Phys. Rev. Lett. **62**, 1197 (1989).
[3] P. Fournier, E. Maiser, and R.L. Greene, in *The Gap Symmetry and Fluctuations in High-Tc Superconductors*, Series B: Physics, Vol. 371, NATO ASI Series, edited by J. Bok (Springer, Berlin, 1998).
[4] T. Timusk and B. Statt, Rep. Prog. Phys. **62**, 61 (1999).
[5] J. Orenstein, G.A. Thomas, A.J. Millis, S.L. Cooper, D.H. Rapkine, T. Timusk, L.F. Schneemeyer, and J.V. Waszczak, Phys. Rev. B **42**, 6342 (1990).
[6] A.V. Puchkov, D.N. Basov, and T. Timusk, J. Phys.: Condens. Matter **8**, 10049 (1996).
[7] A.F. Santander-Syro, R.P.S.M. Lobo, N. Bontemps, Z. Konstantinovic, Z.Z. Li, and H. Raffy, Europhys. Lett. **62**, 568 (2003).
[8] H.J.A. Molegraaf, C. Presura, D. van der Marel, P.H. Kes, and M. Li, Science **295**, 2239 (2002).
[9] C.C. Homes, S.V. Dordevic, D.A. Bonn, R. Liang, and W.N. Hardy, Phys. Rev. B **69**, 024514 (2004).
[10] A. Zimmers, J.M. Tomczak, R.P.S.M. Lobo, N. Bontemps, C.P. Hill, M.C. Barr, Y. Dagan, R.L. Greene, A.J. Millis, and C.C. Homes, cond-mat/0406204 (unpublished).
[11] Y. Onose, Y. Taguchi, K. Ishizaka, and Y. Tokura, Phys. Rev. Lett. **87**, 217001 (2001).
[12] Y. Onose, Y. Taguchi, K. Ishizaka, and Y. Tokura, Phys. Rev. B **69**, 024504 (2004).
[13] C.C. Homes, B.P. Clayman, J.L. Peng, and R.L. Greene, Phys. Rev. B **56**, 5525 (1997).
[14] S. Lupi, P. Maselli, M. Capizzi, P. Calvani, P. Giura, and P. Roy, Phys. Rev. Lett. **83**, 4852 (1999).
[15] E.J. Singley, D.N. Basov, K. Kurahashi, T. Uefuji, and K. Yamada, Phys. Rev. B **64**, 224503 (2001).
[16] C.C. Homes, M. Reedyk, D.A. Cradles, and T. Timusk, Appl. Opt. **32**, 2976 (1993).
[17] C. Kendziora, D. Pelloquin, A. Daignere, P. Fournier, Z.Y. Li, R.L. Greene, A.F. Goncharov, V.V. Struzhkin, R.J. Hemley, and H.K. Mao, Physica C **341–348**, 2189 (2000).
[18] C. Kendziora, B. Nachumia, P. Fournier, Z.Y. Li, R.L. Greene, and D.G. Hinks, Physica C **364-365**, 541 (2001).
[19] G. Blumberg, A. Koitzsch, A. Gozar, B.S. Dennis, C. Kendziora, P. Fournier, and R.L. Greene, Phys. Rev. Lett. **88**, 107002 (2002).
[20] E. Maiser, P. Fournier, J.L. Peng, F.M. Araujo-Moreira, T. Venkatesan, R.L. Greene, and G. Czjzek, Physica C **297**, 15 (1998).
[21] A.F. Santander-Syro, R.P.S.M. Lobo, N. Bontemps, W. Lopera, D. Girata, Z. Konstantinovic, Z.Z. Li, and H. Raffy, Phys. Rev. B **13**, 134504 (2004).
[22] R.A. Ferrell and R.E. Glover, Phys. Rev. **109**, 1398 (1958).
[23] M. Tinkham and R.A. Ferrell, Phys. Rev. Lett. **2**, 331 (1959).
[24] S.V. Dordevic, E.J. Singley, D.N. Basov, S. Komiya, Y. Ando, E. Bucher, C.C. Homes, and M. Strongin, Phys. Rev. B **65**, 134511 (2002).
[25] J.D. Kokales, P. Fournier, L.V. Mercaldo, V.V. Talanov, R.L. Greene, and S.M. Anlage, Phys. Rev. Lett. **85**, 3696 (2000).
[26] A. Snezhko, R. Prozorov, D.D. Lawrie, R.W. Giannetta, J. Gauthier, J. Renaud, and P. Fournier, Phys. Rev. Lett. **92**, 157005 (2004).
[27] M.R. Norman and C. Pépin, Phys. Rev. B **66**, 100506(R) (2002).
[28] J.E. Hirsch and F. Marsiglio, Phys. Rev. B **62**, 15131 (2000).
[29] L. Benfatto, S.G. Sharapov, and H. Beck, Eur. Phys. J. B **39**, 469 (2004).
[30] T. Stanescu and P. Phillips, Phys. Rev. B **69**, 245104 (2004).
[31] J. Ashkenazi, J. Phys. Chem. Solids **65**, 1461 (2004).
[32] J.P. Carbotte and E. Schachinger, Phys. Rev. B **69**, 224501 (2004).